Chapter 6
Crystallization in Nanoparticles

Aurora Nogales and Daniel E. Martínez-Tong

6.1 Introduction

Under particular circumstances, some polymers may crystallize. However, a polymer melt consists of an assembly of polymer chains that are coiled and mutually interpenetrated, and therefore it is impossible to attain an ideal crystalline state of extended straight chains with the endgroups assembled in planar interfaces, purely due to kinetic reasons. The required complete disentangling would need a very long time, as it is associated with an extremely high entropic activation barrier. Instead, a polymer melt cooled below the equilibrium melting point produces a system which is only in part crystalline. Semicrystalline polymers consist of a complex puzzle of crystalline lamellae, crystal-amorphous interphases, stacks of crystalline lamellae, liquid pockets, rigid amorphous phases, and fringed micellar crystals. The arrangement of these structural elements in a given polymer depends on different factors, including chemical structure, chain flexibility, thermal history, and orientation. The structure of semicrystalline polymers exhibits characteristic features depending on the length scales. In the 10^{-8} m scale, in highly crystalline polymers, such as polyethylene (PE) (Wunderlich 1973) and in intermediate crystalline polymers, such as polyethylene terephthalate (PET) (Santa Cruz et al. 1991) or poly(etherketone)s (Bassett et al. 1988), there is an alternation between crystalline regions (lamellar crystals) and amorphous regions (interlamellar amorphous regions). With the exception of highly crystalline polymers, this alternation does not extend to the whole volume of the sample (Santa Cruz et al. 1991). The lamellae are packed into stacks which are separated by broad amorphous regions. The stacks can assemble

A. Nogales (✉) • D.E. Martínez-Tong
Instituto de Estructura de la Materia (IEM-CSIC), C/Serrano 121,
Madrid 28006, Madrid, Spain
e-mail: aurora.nogales@csic.es

G.R. Mitchell, A. Tojeira (eds.), *Controlling the Morphology of Polymers*,
DOI 10.1007/978-3-319-39322-3_6

themselves into superstructures, generally with spherical symmetry (spherulites) which can reach microns or even several millimeters.

Nowadays, current interest in the properties of polymers confined into nanometer scale is very intense, both from the fundamental and practical perspectives (Soles and Ding 2008). Polymers are extensively used in processes to fabricate nano-objects like wires of nanometer-scale diameters (Martín and Mijangos 2009; Chen et al. 2012; Martín et al. 2012) nanoimprinting (Soles and Ding 2008), and nanoscale polymeric particles (Landfester 2001). Confined polymers are central to a broad range of advanced materials and emerging nanotechnologies (Coakley and Mcgehee 2004; Chen et al. 2012), with applications including biomaterials (Yu et al. 2011; Bonanno and Segal 2011), micro- and optoelectronics (Yuan et al. 2011; Tong et al. 2011; Di Benedetto et al. 2008), energy capture/storage (Li et al. 2012; Cai et al. 2012; Li and Malardier-Jugroot 2011; Guan et al. 2011; Mohapatra et al. 2009), among others. Besides cutting-edge fabrication strategies, control over the changes in properties induced by nanoscale confinement is a central issue to be taken into account. The rapid development of nano-science and nanotechnology in the twentieth and twenty-first centuries raises a lot of questions about the structure and surface properties of nano-materials (Svorcik et al. 2013). The prefix ***nano***- is used in a broad way to describe systems where one or several physical dimensions have been reduced to length scales between 1 and 100 nm, and also to the application of concepts and understanding of properties (physical, chemical, biological, mechanical, . . .) that derive as a result of the reduced length scale (Gates et al. 2005; Martín Gago et al. 2008). The possible change in properties, when a material is nanostructured, is understood as ***confinement effects*** (Alcoutlabi and McKenna 2005).

As for smaller molecules (Grigoriadis et al. 2011), crystallization becomes even more sluggish when the chains are confined at the nanoscale level (Vanroy et al. 2013; Liu and Chen 2010). Confinement is able to induce different morphologies (Asada et al. 2012; Maillard and Prud'homme 2008), reduce crystallization rates by several orders of magnitude (Despotopoulou et al. 1996; Massa et al. 2003), and in some cases, inhibition of crystallization within the experimental time scale (Capitán et al. 2004). Therefore, in order to widen the applicability of semicrystalline polymers at the nanoscale, the effect of confinement on the crystallinity and morphology should be considered.

Polymers confined in nanometer-sized geometries have been intensively investigated in the last decades, aiming both to achieve a deeper understanding of finite-size effects in soft matter and to improve the performance of nano-devices and hybrid materials (Napolitano et al. 2013). When designing and preparing nanostructures, one or several physical dimensions can be affected. For example, if a nanostructured polymer system is prepared in a way that two dimensions have macroscopic dimensions, while the remaining is in the nanometer scale, the resulting material is said to be one dimensionally confined (1D-confinement). This is the case of ***polymer thin films***. If two dimensions have nanometer scales, one can talk about two dimensional confinement (2D-confinement), which is the case of ***nanowires*** and nanotubes. Finally, when all three dimensions are in the nanometer length scale,

such as in ***nanoparticles***, the polymer is said to be three-dimensionally confined (3D-confinement). Moreover, confined polymer structures can be further processed to obtain *à la carte* nano-features, such as nanostructured surfaces on polymer thin films (Rebollar et al. 2011), alignment of polymer nanowires by percolation into nanoporous membranes (Garcia-Gutierrez et al. 2013; Martin et al. 2014), or even physical responsive polymer nanoparticles (Deng et al. 2013).

Among the most studied confining geometries are thin films, probably due to their presence in a large number of technological applications, and also because it provides an easy control of the level of confinement and tunability of interfacial interactions between polymers and substrates (Rotella et al. 2011). In this geometry, the sample thickness becomes a crucial parameter controlling crystallization (Vanroy et al. 2013), while surface effects mostly lead to a competition between adsorption to the solid surface and nucleation of polymer crystals (Reiter and Sommer 1998; Vanroy et al. 2013; Napolitano and Wübbenhorst 2007; Asada et al. 2012; Bertoldo et al. 2010). Also, polymer thin films represent highly metastable forms of matter, presenting unexpected properties (Reiter and DE Gennes 2001) which have been widely discussed by the scientific community in the past years (Forrest et al. 1997; Tsui and Zhang 2001; Schönhals et al. 2002; McKenna 2003; Wübbenhorst and Lupascu 2005; Napolitano et al. 2013; Napolitano and Cangialosi 2013; Boucher et al. 2012). It is also possible to attain information of the role of interfacial interactions by intercalating a polymer thin film in between two adsorbing layers (Napolitano et al. 2013) although the introduction of burying interfaces limits the possible experimental protocols; for example, metallization of both polymer faces does not permit an optical access to the polymer surface.

On the other hand, using confined polymers into droplets and nanoparticles might serve as starting point in order to prepare *nanocrystals* and also to better understand the mechanisms involved during nucleation and crystallization in confined geometries (Massa and Dalnoki-Veress 2004; Li 2009) without including any preferential confined dimension. In this chapter, we present the crystallization behavior of polymers in confined nanoparticles.

6.2 Generation of Polymer Nanoparticles

The formation of structured polymeric nanoparticles is of great importance for many applications. In general, polymer nanoparticles can be prepared from several heterophase methods. One of the most known methods, developed extensively by Landfester et al. during the last decade, is the so-called miniemulsion method (Landfester 2001, 2009; Kietzke et al. 2007).

An emulsion consists of well-dispersed droplets of a substance into a continuous phase. This is formed by mixing two immiscible phases that are subjected to high shear, resulting in small, homogeneous, and narrowly distributed nanodroplets. The miniemulsion can be stabilized by means of surfactants. The protocol is sketched in Fig. 6.1.

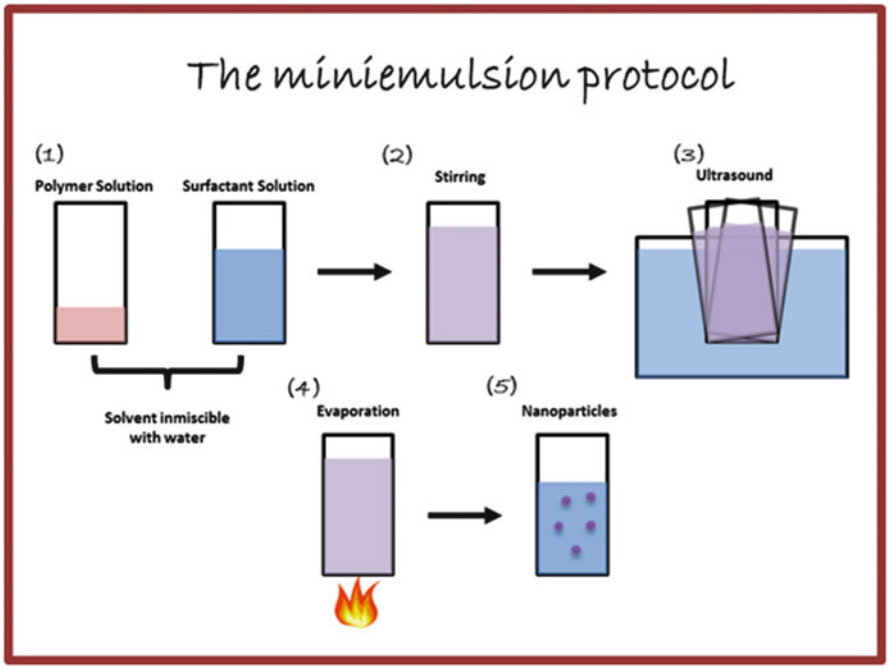

Fig. 6.1 Sketch of the miniemulsion protocol to generate polymer nanoparticles

By using this method, polymer nanoparticles of different polymers have been reported (Martínez-Tong et al. 2013, 2014; Landfester 2001). For amorphous polymers, the shape of the nanoparticles generated by this technique is spherical (Fig. 6.2). Variations of physical properties like the glass transition temperature of the polymer confined into the shape of this nanoparticles have been reported in the literature (Martínez-Tong et al. 2013, 2014).

Another approach for obtaining polymer nanoparticles is the so-called reprecipitation method, previously proposed by Shimizu et al. (2007). This method relays on crashing out hydrophobic polymer chains in solution by displacing a solvent with a non-solvent, generally water. Both polymer solvent and non-solvent must be miscible. As in the miniemulsion technique, reprecipitation can be used by starting from the bulk polymer of known molecular weight as the precursor material; only the nanoparticle diameter needs to be adjusted during the process by controlling solution concentration. The method is schematically described in Fig. 6.3.

Figure 6.4 shows an AFM image of polyethylmethacrylate (PEMA) nanoparticles prepared by reprecipitation.

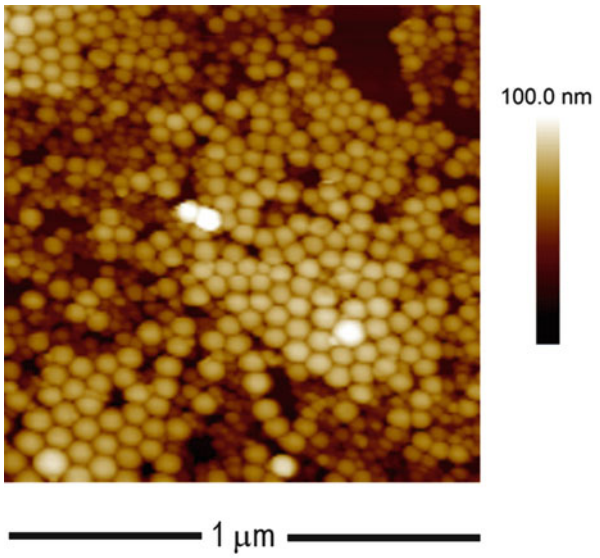

Fig. 6.2 Atomic Force Microscopy (AFM) topography image of polystyrene (PS) nanoparticles prepared by the miniemulsion method after spin casting the miniemulsion on a silicon wafer. The starting material is the bulk polymer

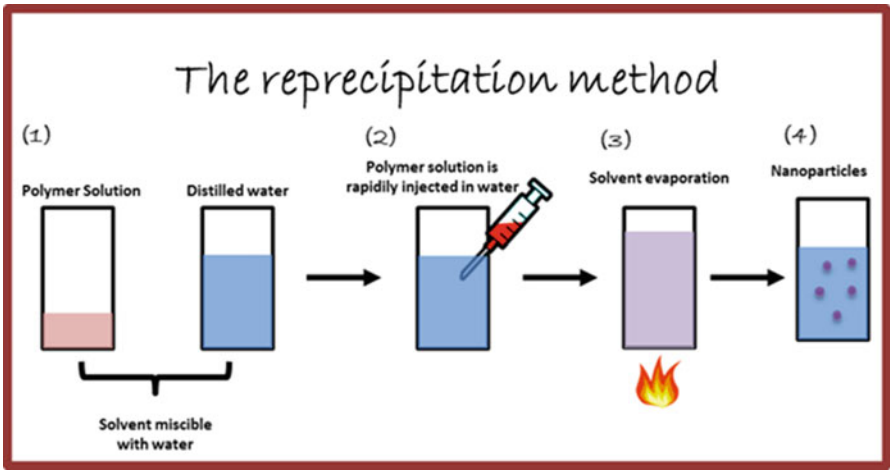

Fig. 6.3 Sketch of the reprecipitation protocol to generate polymer nanoparticles

6.3 Modification of the Crystalline Morphology by Confinement into Nanoparticles

By the two previously mentioned methods it is possible to nanostructure, within the shape of particles, polymers that are either inherently semicrystalline or that are able to crystallize. One example of this type of polymers is poly(lactic acid), from now on abbreviated as PLA. PLA is an aliphatic thermoplastic polymer, commonly

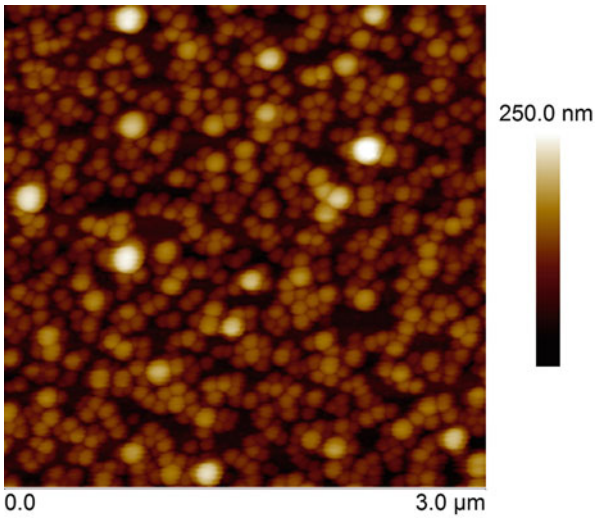

Fig. 6.4 AFM topography image of PEMA nanoparticles prepared by the reprecipitation method after spin casting on a silicon wafer

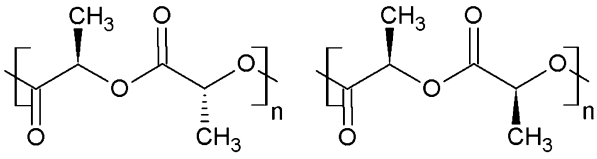

Fig. 6.5 (*Left*) Sketch of a PLLA repeating unit. (*Right*) Sketch of a D,L-dimer

made from α-hydroxy acids which are considered biodegradable, biocompatible, and compostable (Garlotta 2001; Anderson and Shive 2012). Although the term acid is generally included in its name, PLA is a polyester instead of a *polyacid* (Garlotta 2001). Generally, PLA grades are copolymers of poly(L-lactic acid) (PLLA) and poly(D,L-lactic acid) (PDLLA), which are produced from L-lactides and D,L-lactides, respectively (Martin and Avérous 2001). The sketch of these molecules is shown in Fig. 6.5.

The letters D and L are related to Dextrorotation (D) and Levorotation (L) and refer to the polymer property of rotating plane polarized light. If the light rotates clockwise as it approaches an observer, this is known as dextrorotation (light with a rotation to the right). If the light rotates counterclockwise as it approaches the observer, then the light exhibits levorotation (rotation to the left). The ratio of L- to D,L- enantiomers is known to affect the properties of PLA, such as the melting temperature and the degree of crystallinity (Martin and Avérous 2001).

PDLLA (NatureWorks, PLA 2002D, D-content 4.25 %, $\rho = 1.24$ g/cm^3) nanoparticles can be prepared either by the miniemulsion method or the reprecipitation method. In the present case, for the miniemulsion method PDLLA was dissolved in chloroform ($CHCl_3$), at a 0.2 wt% concentration. The polymer solution was added to a 1 wt% aqueous surfactant solution of sodium dodecyl sulfate (SDS). Pre-emulsification was obtained by stirring at room temperature for

60 min and, afterwards, the stirred mixture was ultrasonicated for 15 min in an ultrasound bath. This allowed obtaining a miniemulsion. Evaporation of the organic solvent, under stirring the miniemulsion at 66 °C for 180 min, yields a dispersion of polymeric nanospheres in a non-solvent medium. To eliminate the excess of SDS, suspensions were dialyzed against distilled water, using a dialysis membrane. The size of the obtained nanospheres is governed principally by the concentration of the polymeric solution and by the concentration of the surfactant, as previously reported (Martínez-Tong et al. 2013).

PDLLA nanoparticles were also prepared by the reprecipitation method. Specifically, 15 mg of PDLLA were dissolved in 5 mL of tetrahydrofuran (THF). The solution was left under stirring at room temperature for 30 min. Afterwards, in order to remove any macroscopic residues, the solution was filtered. Finally, the polymer solution was rapidly injected into a beaker filled with distilled water. This emulsion was left under stirring at room temperature for 90 min and then for 120 min at 66 °C to allow complete removal of the solvent. Figure 6.6 shows AFM topography images of the prepared PDLLA nanoparticles.

Figure 6.6a, b show AFM topography images of the PDLLA nanoparticles prepared by the miniemulsion and reprecipitation method, respectively. In both cases, the nanoparticles consist of polymer nanospheres, without signs of

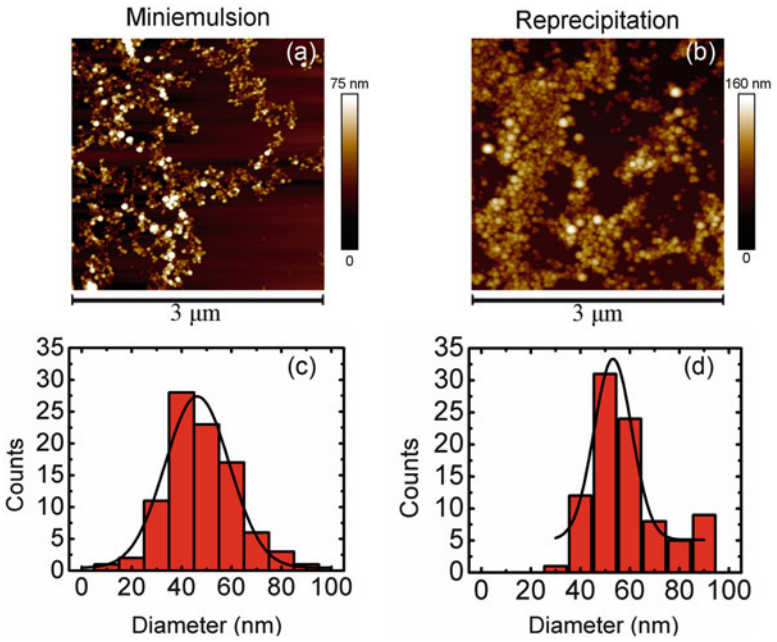

Fig. 6.6 AFM topography images and size distribution of PDLLA nanoparticles prepared by the miniemulsion method (**a**, **c**) and reprecipitation method (**b**, **d**). Size distribution was quantified on the AFM images by measuring the nanoparticles diameters. *Continuous black line* represents a Gaussian fit to the distribution

coalescence and/or ripening. From the AFM images the size distributions of the polymer nanoparticles could be quantified and the results are shown in Fig. 6.6c, d. For both preparation methods, a similar mean value of the PDLLA nanoparticles diameter (d) was found, namely $d_{\text{miniemulsion}} = (46 \pm 1)\,\text{nm}$, and $d_{\text{reprecipitation}} = (53 \pm 3)\,\text{nm}$. To take into consideration the width of the size distributions, it is possible defining a *quality factor* of the resulting nanospheres by $Q = W/\langle d \rangle$, where W is the width of the distribution (nm) and $\langle d \rangle$ is the mean diameter (nm). The closer the factor Q is to zero, the better is the resulting preparation in terms of size monodispersity. In this work, we found small Q values for both preparation methods, $Q_{\text{miniemulsion}} = 0.57 \pm 0.06$ and $Q_{\text{reprecipitation}} = 0.28 \pm 0.07$, indicating that size monodispersity was within acceptable values.

6.3.1 Crystallization in Nanoparticles

Figure 6.7 shows the X-ray diffraction patterns of the nanoparticles, annealed at different temperatures, together with the diffraction from the bulk treated at the same temperatures for comparison. In general, as the samples were annealed, the development of diffraction peaks is evidenced. This indicates that all samples were able to crystallize. Specifically, bulk and miniemulsion nanoparticles patterns are quite similar between each other for the whole temperature range. At 30 °C, these two samples show an amorphous halo, indicating their amorphous nature. As temperature increased up to 70 °C, the development of a diffraction peak, around $2\theta = (17.0 \pm 0.3)°$, is seen. This peak has been reported to be associated with the diffraction from the (200) and/or (110) planes of the α form of PDLLA (Mano et al. 2004). At higher temperatures, the diffraction patterns show the development of several other peaks. This behavior indicates that as the samples were annealed crystallization continues. At 110 °C, diffraction peaks show their highest intensity. Comparing with the literature (Mano et al. 2004; Zhang et al. 2008; Wang et al. 2014; Wei et al. 2014; Wasanasuk et al. 2011), we have indexed the peaks as shown at the 110 °C temperature in Fig. 6.7. Results show that the PDLLA has crystallized in the ordered α-phase (Wei et al. 2014; Xiong et al. 2013; Wasanasuk et al. 2011), which is expected when the polymer is crystallized at temperatures below 100 °C. Indexing results are summarized in Table 6.1.

The diffraction patterns of PDLLA reprecipitation nanoparticles are shown in the right column of Fig. 6.7. In this case, patterns are noisier in comparison to the others. This might be related to the amount of material enclosed in the aluminum sheets, which in this case was lesser. As stated previously, as temperature increases crystallization evolves; however, comparing with bulk and miniemulsion nanoparticles there are important differences. At 30 °C, besides the amorphous halo, an increase of the diffraction signal is observed at small values of 2θ (2°–5°). This result can be related to the possible existence of some ordering in the PDLLA chains within the nanoparticles, which lengthscale is above of WAXS range. It has been reported that poly(lactic acid) polymers can show a mesophase (Zhang

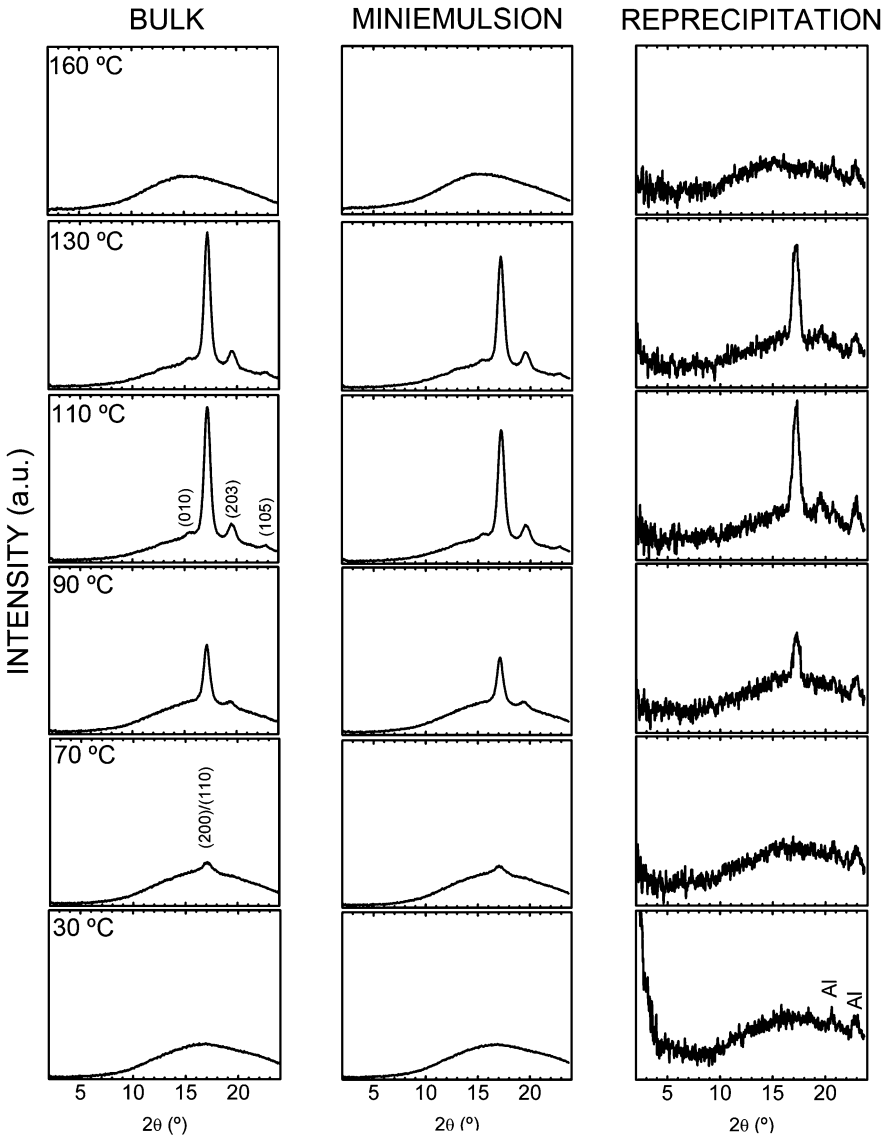

Fig. 6.7 Wide Angle X-ray Scattering (WAXS) diffraction patterns for bulk PDLLA (*left*) and PDLLA miniemulsion (*center*) and reprecipitation (*right*) nanoparticles

Table 6.1 Crystalline peaks and 2θ position, as observed at 130 °C (Fig. 6.7)

Index	Bulk	Miniemulsion	Reprecipitation
(010)	$(15.4 \pm 0.3)^\circ$	$(15.3 \pm 0.3)^\circ$	–
(200)/(110)	$(17.0 \pm 0.3)^\circ$	$(17.1 \pm 0.3)^\circ$	$(17.2 \pm 0.3)^\circ$
(203)	(19.5 ± 0.5)	(19.5 ± 0.5)	(19.5 ± 0.5)
(105)	$(22.7 \pm 0.3)^\circ$	$(22.7 \pm 0.3)^\circ$	$(22.8 \pm 0.3)^\circ$

et al. 2010; Wasanasuk and Tashiro 2011), with distinct chain packing and chain conformation. Mesophases in semicrystalline polymers can be obtained by the melt-quenched methods (Strobl 2006); for example, isotactic polypropylene can be solidified into an intermediate state between crystal and amorphous states when a thin specimen of molten state is rapidly quenched (Qiu et al. 2007). Also, Stoclet and collaborators have shown that it is possible to induce a mesophase in PDLLA when an external strain was applied (Stoclet et al. 2010a, b). Collecting all these facts, we argue that the preparation procedure used in the reprecipitation method might have led to the formation of a mesophase in the resulting PDLLA nanoparticles. We recall that in this method, the polymer solution is rapidly injected into a non-solvent. In the solution, the polymer chains have maximum mobility, which can be somehow compared to the behavior in the melt state. As the solvent is quickly removed from the nanoparticles, while the polymer is being transferred to a non-solvent medium (chains have no mobility), it is possible to assume that the polymer chains are being subjected to a quenching-like procedure that ultimately leads to the formation of the mesophase. It can also be argued that during the fast precipitation, the polymer chains retain residual stresses and thus a sort of strain-induced mesophase takes place. These strains could arise from the physical procedure involved in going from separated chains to nanospheres.

The preparation method argument just explained can be also justified by comparing the results between reprecipitation and miniemulsion PDLLA nanoparticles. In the miniemulsion method, nanodroplets of solvent/polymer are formed simultaneously during ultrasonication. After the formation, solvent is slowly evaporated and thus nanoparticles do not suffer a melt-quench like procedure. Also, the solvent/polymer nanodroplets serve as precursors to the resulting polymer nanoparticles and thus, during solvent evaporation process, polymer chains have enough mobility to lose possible strains. Since the solvent is evaporated at a temperature in which no Bragg peaks are observed, and since there is not enough mobility to crystallize, the resulting nanoparticles are amorphous, without any mesophases.

The WAXS signature of the *so-called mesophase* in the PDLLA reprecipitation nanoparticles vanishes with temperature, in the range 30–60 °C. At 70 °C (Fig. 6.7) the increase a low 2θ is not observed anymore. Figure 6.8 shows the Differential Scanning Calorimetry (DSC) trace of the reprecipitation nanoparticles. Glass transition (T_g), crystallization and melting temperatures are highlighted throughout the curve.

The glass transition temperature of the nanoparticles is observed around 60 °C indicating no change in comparison to the bulk (Bitinis et al. 2011). Comparing WAXS and DSC results, we observe that the mesophase signature in the diffraction pattern disappears at temperatures above T_g. Also, in the DSC curve, just below T_g an endothermic peak can be seen, highlighted with the symbol *. DSC endothermic peaks in semi-crystalline polymers are related to first-order transitions, such as the melting of the crystalline structure. Gathering results, it is possible to speculate that this peak is related to the disordering of the polymer chains in the mesophase, that happens just when the polymer start getting mobility due to the incipient glass

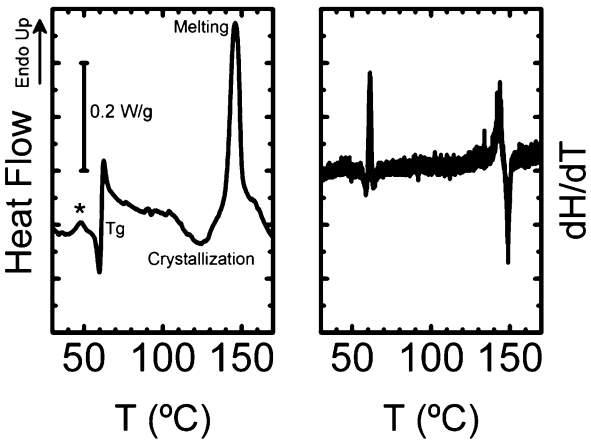

Fig. 6.8 DSC trace (*left*) and heat flow derivative (*right*) of the reprecipitation PDLLA nanoparticles

transition. At temperatures above T_g, the calorimetric curve shows a crystallization peak. The onset of crystallization can be observed around 90 °C and its maximum at 125 °C. Finally, the polymer nanoparticles melt at 145 °C. DSC results of crystallization and melting of the nanoparticles agree with the WAXS patterns.

6.3.2 From Polymer Nanoparticles to Polymer Nanocrystals

WAXS results in the previous section showed that polymer nanoparticles of PDLLA were able to crystallize when heated above certain temperatures. The diffraction patterns also show that nanoparticles prepared via the miniemulsion protocol showed a crystallization behavior quite similar to the bulk polymer. Based on these results, we have evaluated the morphological change of PDLLA nanoparticles prepared by the miniemulsion method, when subjected to thermal treatments.

Figure 6.9 shows (3 × 3) μm AFM topography images of the deposited PDLLA nanoparticles annealed at 75 °C for different times (t). This temperature is above T_g of the PDLLA and according to the WAXS patterns crystallization must take place. Annealing was performed on a hot stage, by heating the Si wafers on where the particles were originally deposited. Each annealing treatment was carried out on independent wafers.

Image at $t = 0$ s corresponds to the deposited nanoparticles without annealing, showing their spherical geometry. After annealing for 5 min, the nanoparticles lose their spherical shape, turning into *islands*, which show a bigger diameter and lower height in comparison to the original nanoparticles. This is an indication of agglomeration and coalescence of neighbor particles, as previously reported for nanospheres of amorphous polymers, where the height:width ratio increased from 1:1 to 1:5 (Martínez-Tong et al. 2013, 2014). The morphology of the nanoparticles

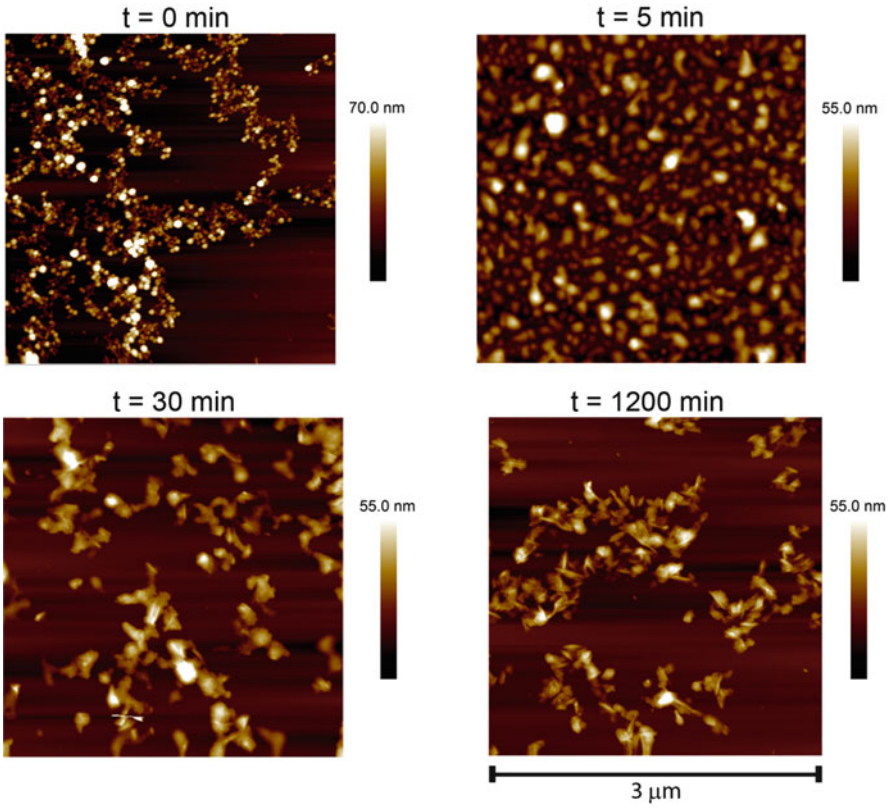

Fig. 6.9 AFM images of PDLLA nanoparticles prepared by the miniemulsion protocol, annealed at 75 °C for different times (*t*)

suffers further changes after 30 min at 75 °C. As time increases, the original smooth edges of the islands observed at 5 min start reshaping into well-defined straight contours. Also, in some cases it is possible to see the appearance of needle-like features inside the nanoparticles. This fact is enhanced at the longest annealing time (1200 min).

Figure 6.10 shows a $(1 \times 1)\,\mu m$ AFM topography image of the PDLLA nanoparticles annealed at 75 °C for 1200 min. In this case, a smaller scan was used (in comparison to images in Fig. 6.9), which allowed getting more insight into the details of the nanocrystals. As stated before, the original spherical nanoparticles present now well-defined edges, as expected for crystalline structures. These crystalline structures seem to be formed by the agglomeration of several nanoparticles, since at the chosen annealing temperature PDLLA is expected to have mobility. Two different structures are observed in the AFM image of Fig. 6.10. First, needle-like crystals (red arrow) resemble the edge-on crystalline structures in

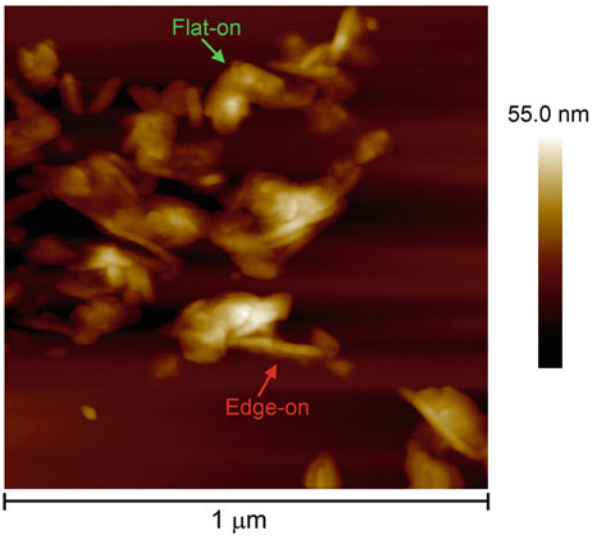

Fig. 6.10 AFM topography image of PDLLA nanoparticles annealed at 75 °C for 1200 min

polymer thin films. On the other hand, the green arrow highlights the structures resembling flat-on crystals, compared to thin polymer films (Wang et al. 2008; Xu et al. 2005).

The needle-like crystals prepared from the PDLLA nanoparticles show widths between 15 and 25 nm, heights between 15 and 40 nm and lengths between 100 and 300 nm. On the other hand, flat-on like crystals show sides between 50 and 150 nm and heights in the 15–60 nm range. Based on the geometrical sizes of the crystals obtained from the PDLLA nanoparticles, it is possible to consider them as ***nanocrystals***. In principle, these nanocrystals could be recovered from the silicon waffers by washing it in distilled water. Afterwards, they could be used as additives in composites and/or polymer blends. Also, the heights of these nanostructures are comparable to the ones obtained for ultra-thin films of PLLA (Maillard and Prud'homme 2008). This allows thinking in possible comparisons in the crystallization between the two confined geometries.

6.4 Summary

We have shown that by various physicochemical methods it is possible to nanostructure bulk polymers in the shape of nanoparticles, that in the case of amorphous polymers, have spherical shape. If the original bulk polymer is able to crystallize, the shape of the nanoparticle is modified by the process of crystallization. However, it is possible to limit the size of the crystal due to the confinement imposed by the nanoparticle shape.

6.5 Methods

Atomic Force Microscopy (AFM). Size and shape of the polymer nanoparticles were characterized by atomic force microscopy (AFM). Samples were drop casted on (100) Si wafers. A Multimode 8 AFM with a Nanoscope V controller (Bruker) was used under tapping mode with NCHV probes (Bruker). Square images with 512×512 pixels resolution were taken. Analysis of size and shape of nanoparticles was performed with the Nanoscope Analysis 1.50 software (Bruker).

Wide Angle X-ray Scattering (WAXS). 2D-WAXS investigations were carried out in transmission geometry using a Bruker AXS Nanostar X-ray scattering instrument. The instrument uses CuKα radiation (1.54 Å) produced in a sealed tube. The sample chamber was under vacuum and controlled temperature. For WAXS experiments, we used lyophilized nanoparticles packed in aluminum sheets. Bulk sample was measured as received also packed in aluminum sheets. The scattered X-rays were detected on a two-dimensional multiwire area detector (Bruker Hi-Star) and converted to one-dimensional scattering by radial averaging and represented as a function of the momentum transfer vector q ($=4\pi/\lambda \sin \theta$) in which θ is half the scattering angle and λ the wavelength of the incident X-ray beam. The sample-to-detector distance was 10 cm. Patterns were collected during 5 min at each temperature.

Differential Scanning Calorimetry (DSC). Calorimetric measurements were carried out by means of a Perkin-Elmer DSC8500 instrument equipped with an Intracooler 2 sub-ambient device and calibrated with purity indium standards. In order to measure the transitions of the nanoparticles, the external block temperature was set at -100 °C. A lyophilized solid powder of nanoparticles was used as sample with weight *c.a.* 2 mg. The powder was enclosed in aluminum pans and heated from -20 to 200 °C at a rate of 20 °C/min. Bulk sample was measured as received, enclosed in aluminum pans.

Bibliography

Alcoutlabi M, McKenna GB (2005) Effects of confinement on material behaviour at the nanometre size scale. J Phys Condens Matter 17:R461

Anderson JM, Shive MS (2012) Biodegradation and biocompatibility of PLA and PLGA microspheres. Adv Drug Deliv Rev 64(Suppl):72–82

Asada M, Jiang N, Sendogdular L, Gin P, Wang Y, Endoh MK, Koga T, Fukuto M, Schultz D, Lee M, Li X, Wang J, Kikuchi M, Takahara A (2012) Heterogeneous lamellar structures near the polymer/substrate interface. Macromolecules 45:7098–7106

Bassett DC, Olley RH, Al Raheil IAM (1988) On crystallization phenomena in PEEK. Polymer 29:1745–1754

Bertoldo M, Labardi M, Rotella C, Capaccioli S (2010) Enhanced crystallization kinetics in poly(ethylene terephthalate) thin films evidenced by infrared spectroscopy. Polymer 51:3660–3668

Bitinis N, Verdejo R, Cassagnau P, Lopez-Manchado MA, Lopez Manchado MA (2011) Structure and properties of polylactide/natural rubber blends. Mater Chem Phys 129:823–831
Bonanno LM, Segal E (2011) Nanostructured porous silicon-polymer-based hybrids: from biosensing to drug delivery. Nanomedicine 6:1755–1770
Boucher VM, Cangialosi D, Yin H, Schonhals A, Alegria A, Colmenero J (2012) Tg depression and invariant segmental dynamics in polystyrene thin films. Soft Matter 8:5119–5122
Cai YB, Gao CT, Xu XL, Fu Z, Fei XZ, Zhao Y, Chen Q, Iu XZ, Wei QF, He GF, Fong H (2012) Electrospun ultrafine composite fibers consisting of lauric acid and polyamide 6 as form-stable phase change materials for storage and retrieval of solar thermal energy. Solar Energy Mater Solar Cell 103:53–61
Capitán MJ, Rueda DR, Ezquerra TA (2004) Inhibition of the crystallization in nanofilms of poly (3-hydroxybutyrate). Macromolecules 37:5653–5659
Chen D, Zhao W, Russell TP (2012) P3HT nanopillars for organic photovoltaic devices nanoimprinted by AAO templates. ACS Nano 6:1479–1485
Coakley KM, Mcgehee MD (2004) Conjugated polymer photovoltaic cells. Chem Mater 16:4533–4542
Deng R, Liang F, Li W, Yang Z, Zhu J (2013) Reversible transformation of nanostructured polymer particles. Macromolecules 46:7012–7017
Despotopoulou MM, Miller RD, Rabolt JF, Frank CW (1996) Polymer chain organization and orientation in ultrathin films: a spectroscopic investigation. J Polym Sci B 34:2335–2349
Di Benedetto F, Camposeo A, Pagliara S, Mele E, Persano L, Stabile R, Cingolani R, Pisignano D (2008) Patterning of light-emitting conjugated polymer nanofibres. Nat Nanotechnol 3:614–619
Forrest JA, Dalnoki-Veress K, Dutcher JR (1997) Interface and chain confinement effects on the glass transition temperature of thin polymer films. Phys Rev E 56:5705
Garcia-Gutierrez M-C, Linares A, Martin-Fabiani I, Hernandez JJ, Soccio M, Rueda DR, Ezquerra TA, Reynolds M (2013) Understanding crystallization features of P(VDF-TrFE) copolymers under confinement to optimize ferroelectricity in nanostructures. Nanoscale 5:6006–6012
Garlotta D (2001) A literature review of poly(lactic acid). J Polym Environ 9:63–84
Gates BD, Xu Q, Stewart M, Ryan D, Willson CG, Whitesides GM (2005) New approaches to nanofabrication: molding, printing, and other techniques. Chem Rev 105:1171–1196
Grigoriadis C, Duran H, Steinhart M, Kappl M, Butt H-J, Floudas G (2011) Suppression of phase transitions in a confined rodlike liquid crystal. ACS Nano 5:9208–9215
Guan FX, Wang J, Yang LY, Tseng JK, Han K, Wang Q, Zhu L (2011) Confinement-induced high-field antiferroelectric-like behavior in a poly(vinylidene fluoride-co-trifluoroethylene-co-chlorotrifluoroethylene)-graft-polystyrene graft copolymer. Macromolecules 44:2190–2199
Kietzke T, Neher D, Kumke M, Ghazy O, Ziener U, Landfester K (2007) Phase separation of binary blends in polymer nanoparticles. Small 3:1041–1048
Landfester K (2001) The generation of nanoparticles in miniemulsions. Adv Mater 13:765–768
Landfester K (2009) Miniemulsion polymerization and the structure of polymer and hybrid nanoparticles. Angew Chem Int Ed 48:4488–4507
Li CY (2009) Polymer single crystal meets nanoparticles. J Polym Sci B 47:2436–2440
Li X, Malardier-Jugroot C (2011) Synthesis of polypyrrole under confinement in aqueous environment. Mol Simul 37:694–700
Li JJ, Tan SB, Ding SJ, Li HY, Yang LJ, Zhang ZC (2012) High-field antiferroelectric behaviour and minimized energy loss in poly(vinylidene-co-trifluoroethylene)-graft-poly(ethyl methacrylate) for energy storage application. J Mater Chem 22:23468–23476
Liu Y-X, Chen E-Q (2010) Polymer crystallization of ultrathin films on solid substrates. Coord Chem Rev 254:1011–1037
Maillard D, Prud'homme RE (2008) Crystallization of ultrathin films of polylactides: from chain chirality to lamella curvature and twisting. Macromolecules 41:1705–1712
Mano JF, Wang Y, Viana JC, Denchev Z, Oliveira MJ (2004) Cold crystallization of PLLA studied by simultaneous SAXS and WAXS. Macromol Mater Eng 289:910–915

Martin O, Avérous L (2001) Poly(lactic acid): plasticization and properties of biodegradable multiphase systems. Polymer 42:6209–6219

Martin J, Campoy-Quiles M, Nogales A, Garriga M, Alonso MI, Goni AR, Martin-Gonzalez M (2014) Poly(3-hexylthiophene) nanowires in porous alumina: internal structure under confinement. Soft Matter 10:3335–3346

Martín J, Mijangos C (2009) Tailored polymer-based nanofibers and nanotubes by means of different infiltration methods into alumina nanopores. Langmuir 25:1181–1187

Martín J, Maiz J, Sacristan J, Mijangos C (2012) Tailored polymer-based nanorods and nanotubes by "template synthesis": from preparation to applications. Polymer 53:1149–1166

Martín Gago JA, Briones Llorente C, Casero Junquera E, Serena Domingo PA (2008) Nanotecnologia y Nanociencia: Entre la ciencia ficción del presente y la tecnología del futuro. Fundación Española para la Ciencia y la Tecnología, Madrid

Martínez-Tong DE, Soccio M, Sanz A, García C, Ezquerra TA, Nogales A (2013) Chain arrangement and glass transition temperature variations in polymer nanoparticles under 3D-confinement. Macromolecules 46:4698–4705

Martínez-Tong DE, Cui J, Soccio M, García C, Ezquerra TA, Nogales A (2014) Does the glass transition of polymers change upon 3D confinement? Macromol Chem Phys 215:1620–1624

Massa MV, Dalnoki-Veress K (2004) Homogeneous crystallization of poly(ethylene oxide) confined to droplets: the dependence of the crystal nucleation rate on length scale and temperature. Phys Rev Lett 92:255509

Massa MV, Dalnoki-Veress K, Forrest JA (2003) Crystallization kinetics and crystal morphology in thin poly(ethylene oxide) films. Eur Phys J E 11:191–198

McKenna GB (2003) Status of our understanding of dynamics in confinement: perspectives from confit 2003. Eur Phys J E 12:191

Mohapatra SR, Thakur AK, Choudhary RNP (2009) Effect of nanoscopic confinement on improvement in ion conduction and stability properties of an intercalated polymer nanocomposite electrolyte for energy storage applications. J Power Sources 191:601–613

Napolitano S, Cangialosi D (2013) Interfacial free volume and vitrification: reduction in Tg in proximity of an adsorbing interface explained by the free volume holes diffusion model. Macromolecules 46:8051–8053

Napolitano S, Wübbenhorst M (2007) Deviation from bulk behaviour in the cold crystallization kinetics of ultrathin films of poly(3-hydroxybutyrate). J Phys Condens Matter 19:205121

Napolitano S, Capponi S, Vanroy B (2013) Glassy dynamics of soft matter under 1D confinement: how irreversible adsorption affects molecular packing, mobility gradients and orientational polarization in thin films. Eur Phys J E 36:1–37

Qiu J, Wang Z, Yang L, Zhao J, Niu Y, Hsiao BS (2007) Deformation-induced highly oriented and stable mesomorphic phase in quenched isotactic polypropylene. Polymer 48:6934–6947

Rebollar E, Pérez S, Hernández JJ, Martín-Fabiani I, Rueda DR, Ezquerra TA, Castillejo M (2011) Assessment and formation mechanism of laser-induced periodic surface structures on polymer spin-coated films in real and reciprocal space. Langmuir 27:5596–5606

Reiter G, de Gennes PG (2001) Spin-cast, thin, glassy polymer films: highly metastable forms of matter. Eur Phys J E 6:25

Reiter G, Sommer J-U (1998) Crystallization of adsorbed polymer monolayers. Phys Rev Lett 80:3771

Rotella C, Wübbenhorst M, Napolitano S (2011) Probing interfacial mobility profiles via the impact of nanoscopic confinement on the strength of the dynamic glass transition. Soft Matter 7:5260

Santa Cruz C, Stribeck N, Zachmann HG, Balta Calleja FJ (1991) Novel aspects in the structure of poly(ethylene terephthalate) as revealed by means of small angle x-ray scattering. Macromolecules 24:5980–5990

Schönhals A, Goering H, Schick C (2002) Segmental and chain dynamics of polymers: from the bulk to the confined state. J Non Cryst Solids 305:140

Shimizu H, Yamada M, Wada R, Okabe M (2007) Preparation and characterization of water self-dispersible poly(3-hexylthiophene) particles. Polym J 40:33–36
Soles CL, Ding Y (2008) Nanoscale polymer processing. Science 322:689–690
Stoclet G, Seguela R, Lefebvre JM, Elkoun S, Vanmansart C (2010a) Strain-induced molecular ordering in polylactide upon uniaxial stretching. Macromolecules 43:1488–1498
Stoclet G, Seguela R, Lefebvre JM, Rochas C (2010b) New Insights on the strain-induced mesophase of poly(d, l-lactide): in situ WAXS and DSC study of the thermo-mechanical stability. Macromolecules 43:7228–7237
Strobl G (2006) Crystallization and melting of bulk polymers: new observations, conclusions and a thermodynamic scheme. Prog Polym Sci 31:398–442
Svorcik V, Slepicka P, Siegel J, Reznickova A, Lyutakov O, Kvitek O, Hubacek T, Slepickova Kasalkova N, Kolska Z (2013) Nanostructuring of solid surfaces. In: Dong Y (ed) Nanostructures: properties, production methods and applications. Nova Science Publishers, Hauppauge, NY
Tong L, Cheng BW, Liu ZS, Wang Y (2011) Fabrication, structural characterization and sensing properties of polydiacetylene nanofibers templated from anodized aluminum oxide. Sens Actuat B Chem 155:584–591
Tsui OKC, Zhang HF (2001) Effects of chain ends and chain entanglement on the glass transition temperature of polymer thin films. Macromolecules 34:9139
Vanroy B, Wübbenhorst M, Napolitano S (2013) Crystallization of thin polymer layers confined between two adsorbing walls. ACS Macro Lett 2:168
Wang Y, Chan C-M, Ng K-M, Li L (2008) What controls the lamellar orientation at the surface of polymer films during crystallization? Macromolecules 41:2548–2553
Wang Y, Li M, Wang K, Hao C, Li Q, Shen C (2014) Unusual structural evolution of poly(lactic acid) upon annealing in the presence of an initially oriented mesophase. Soft Matter 10:1512–1518
Wasanasuk K, Tashiro K (2011) Structural regularization in the crystallization process from the glass or melt of poly(l-lactic acid) viewed from the temperature-dependent and time-resolved measurements of FTIR and wide-angle/small-angle X-ray scatterings. Macromolecules 44:9650–9660
Wasanasuk K, Tashiro K, Hanesaka M, Ohhara T, Kurihara K, Kuroki R, Tamada T, Ozeki T, Kanamoto T (2011) Crystal structure analysis of poly(l-lactic acid) α form on the basis of the 2-dimensional wide-angle synchrotron X-ray and neutron diffraction measurements. Macromolecules 44:6441–6452
Wei X-F, Bao R-Y, Cao Z-Q, Zhang L-Q, Liu Z-Y, Yang W, Xie B-H, Yang M-B (2014) Greatly accelerated crystallization of poly(lactic acid): cooperative effect of stereocomplex crystallites and polyethylene glycol. Colloid Polym Sci 292:163–172
Wübbenhorst M, Lupascu V (2005) Glass transition effects in ultra-thin polymer films studied by dielectric spectroscopy—chain confinement vs. finite size effects. In: 12th international symposium on electrets, p 87
Wunderlich B (1973) Macromolecular physics, vol 1: crystal structure, morphology, defects. Academic, New York
Xiong Z, Liu G, Zhang X, Wen T, DE Vos S, Joziasse C, Wang D (2013) Temperature dependence of crystalline transition of highly-oriented poly(l-lactide)/poly(d-lactide) blend: in-situ synchrotron X-ray scattering study. Polymer 54:964–971
Xu J, Guo B-H, Zhou J-J, Li L, Wu J, Kowalczuk M (2005) Observation of banded spherulites in pure poly(l-lactide) and its miscible blends with amorphous polymers. Polymer 46:9176–9185
Yu DG, Branford-White C, Williams GR, Bligh SWA, White K, Zhu LM, Chatterton NP (2011) Self-assembled liposomes from amphiphilic electrospun nanofibers. Soft Matter 7:8239–8247
Yuan K, Li F, Chen YW, Wang XF, Chen L (2011) In situ growth nanocomposites composed of rodlike ZnO nanocrystals arranged by nanoparticles in a self-assembling diblock copolymer for heterojunction optoelectronics. J Mater Chem 21:11886–11894

Zhang J, Tashiro K, Tsuji H, Domb AJ (2008) Disorder-to-order phase transition and multiple melting behavior of poly(l-lactide) investigated by simultaneous measurements of WAXD and DSC. Macromolecules 41:1352–1357

Zhang J, Duan Y, Domb AJ, Ozaki Y (2010) PLLA mesophase and its phase transition behavior in the PLLA−PEG−PLLA copolymer as revealed by infrared spectroscopy. Macromolecules 43:4240–4246